

Reconfigurable 2×1 CPW-Fed Rectangular Slot Antenna Array (RSAA) Based on Graphene for Wireless Communications

Dalia M. Elsheakh^{1,2} and Osama M. Dardeer²

¹Electrical Dept., Faculty of Engineering and Technology, Badr University in Cairo, Egypt
dalia-mohamed@buc.edu.eg / daliaelsheakh@eri.sci.eg

²Microstrip Dept., Electronics Research Institute, 11843, El Nozha, Cairo, Egypt

Abstract— This article presents a 2×1 CPW ultra wideband rectangular slot antenna array (UWB-RSAA) with a modified circular slot shape to support a high data rate for wireless communications applications. The proposed antenna array dimensions are $0.7\lambda_0 \times 0.8\lambda_0 \times 0.064\lambda_0$ at the resonant frequency 1.8 GHz. It is fabricated on Rogers RO4003 substrate and fed by using a coplanar waveguide (CPW). A graphene layer is added on one side of the substrate to realize frequency reconfigurability and improve the array gain. The proposed array acquires -10 dB impedance bandwidth of the RSAA that extends from 1.7 GHz to 2.6 GHz, from 3.2 to 3.8 GHz, and from 5.2 GHz to 7 GHz. The proposed array achieved a realized peak gain of 7.5 dBi at 6.5 GHz at 0 Volt bias with an average gain of 4.5 dBi over the operating band. When the graphene bias is increased to 20 Volt, the antenna bandwidth extends from 1 GHz to 4 GHz and from 5 to 7 GHz with a peak gain of 14 dBi at 3.5 GHz and an average gain of 7.5 dBi. The linearly polarized operation of the proposed array over the operating bands makes it suitable for short-range wireless communications.

Index Terms — Antenna array, detection and wireless communication applications, graphene, reconfigurable.

I. INTRODUCTION

Frequency tuning of the microwave systems has gained a great attention in the research field of antennas and wireless communications. Reconfigurable antenna array is one of the most important elements of the RF circuits [1-4]. In addition, the reconfigurable UWB antennas array could be served several selected frequency bands to avoid the unwanted frequencies and frequency fading. However, integrated RF systems needs reconfigurable antennas less space [6-7]. Several techniques have been reported in literature to achieve reconfigurability in the array operation. This includes using varactor diodes [8], PIN diodes [9], MEMS [10], and other techniques [11, 12].

Graphene is one of the most important materials in

21st century with superior electrical properties that can fit different applications. Graphene sheet is honeycomb lattice arrangement of carbon atoms as reported in early investigations at 2004 in 2004 [13]. Many researches have reported graphene applications for radio frequency (RF), microwave (MW), millimeter wave (MM) and terahertz (THz) applications in [14–15]. One of the most effective research areas utilized graphene sheet layer for steering radiation pattern based on its tunable conductivity [16]. Tuning the conductivity of Graphene is based on changing the applied DC bias voltage, which varies the chemical potential [17]. Several reports in the literature present a fabrication of high-quality graphene with controlled properties. So, great efforts have been made in this area for designing frequency reconfigurable antenna arrays [18–21].

In this paper, reconfigurable 2×1 CPW-fed RSAA as shown in Fig. 1 with an acceptable gain is introduced for different wireless communications applications. The antenna array is fed by 3-dB CPW power divider, which makes the structure easy to integrate with other microwave circuits. A graphene pad layer is placed below the feeding network to achieve the frequency reconfigurability action.

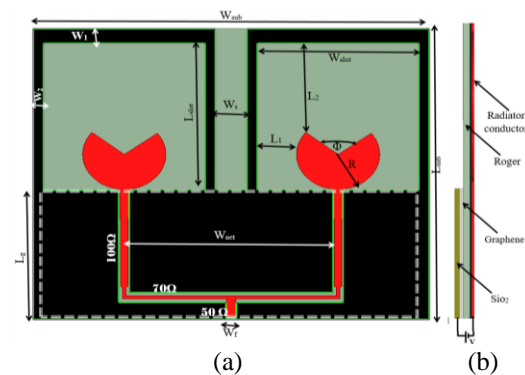


Fig. 1. (a) The structure geometry of the proposed 2×1 RSAA, and (b) side view.

This article is organized as follows; Section I introduces the idea of the paper while section II presents the proposed RSAA design. Section III discusses the graphene layer structure and its properties, then the experimental setup and results are presented in Section IV. After that section V illustrates the group delay results and object detection application and finally Section IV concludes and summarizes the results of the paper.

II. DESIGN OF THE ANTENNA ARRAY

The CPW-fed proposed antenna array is printed on a dielectric substrate Rogers RO4003 with a dielectric constant of 3.5 and a loss tangent of 0.0012. The substrate has dimensions ($L_{\text{sub}} \times W_{\text{sub}}$) of $100 \times 115 \text{ mm}^2$, and a thickness of 0.8 mm. CPW fed slot antennas are very popular and exhibit broad bandwidth and appropriate gain [23]. First design is a conventional 2×1 circular shape of monopole antenna array, which is fed using 3-dB power divider and CPW-fed network as shown in Fig. 2 (a) [24]. The reflection coefficient $|S_{11}|$ of proposed array is shown in Fig. 3 as dash red line. From Fig. 3 (a) the array starts to operate at 3 GHz at reflection impedance bandwidth $\leq -10 \text{ dB}$. Then quarter of the circular shape is etched as shown in Fig. 2 (b) to broaden the bandwidth and the resonant frequency is reduced to 2.5 GHz as shown in Fig. 3 (black line). The rectangular strip is added around the antenna circular shape as shown in Fig. 2 (c) to achieve ultra-wideband impedance bandwidth as shown in Fig. 3 (blue dash dot line), and the array resonant frequency is shifted downwards to operate at 1.7 GHz with improved gain. Figure 3 shows the reflection coefficient variation versus frequency for the prototypes in Fig.3.

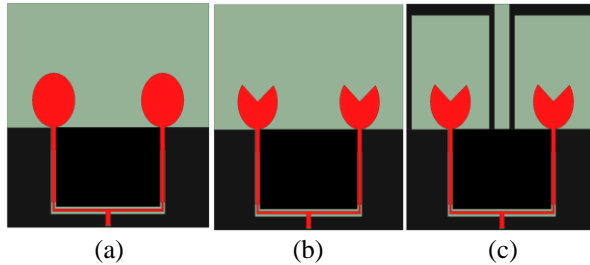


Fig. 2. The design steps of 2×1 array: (a) circular monopole, (b) modified circular, and (c) slot antenna array.

The results illustrate the bandwidth improvement after each step of the design. The complete optimized dimensions of the 2×1 antenna array are shown in Table 1. In addition, the current distribution at different resonant frequencies of the RSAA are shown in Fig. 4. The highest magnitude of the current represent the corresponding elements of the radiation.

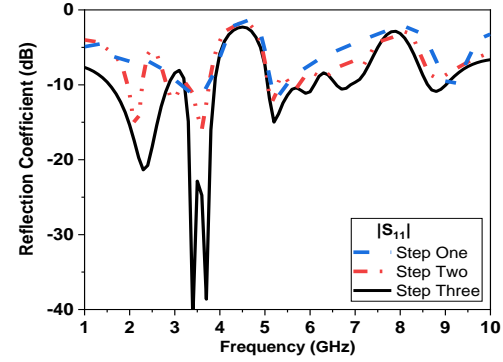


Fig. 3. $|S_{11}|$ versus frequency for the design steps of the proposed antenna array.

III. MODEL OF GRAPHENE ANTENNA

The design of antenna arrays plays a significant role in achieving high gain in a certain specified direction [13]. Moreover, multiband designs offer an excellent opportunity to the system to serve more applications with the same physical components. The previous section described the proposed 2×1 antenna array. However, this section will describe the addition of two graphene layers (on the other side of the substrate) between the Roger substrate and silicon oxide substrate to realize reconfigurable operation in the operating frequency.

A. Graphene conductivity variation

Graphene oxide (GO) has become important material as a result of its low cost, various simple preparation techniques that can be easily transformed to commercial graphene as RGO (reduced graphene oxide) [25-26]. 2D Graphene sheet is a material composed of highly conductive films with high mobility of $0.2 \text{ Mm}^2\text{v}^{-1}\text{sec}^{-1}$ to enhance the antenna performance [27-28], [30]. Graphene sheet has a tunable conductivity of about 10 S/m in the case of 20 voltage bias and about 1000 S/m in the case of zero voltage as shown in Fig. 5. The equivalent circuit model of the graphene layer is an as impedance R_g and inductor L_g in series. The values of graphene impedance vary according to the applied bias voltage as shown in Fig. 6. The change in the graphene properties results in changes in its resistance and inductance as shown in Fig. 6. This could be attributed to design an antenna with tunable operating frequency [31-34]. In this method at such case, the operating frequency is defined where the antenna exhibits the best input matching. Moreover, the maximum gain could be adjusted electronically by modifying the voltage applied to graphene sheet:

$$Z_s = \frac{1}{\sigma} \quad (1)$$

$$\sigma = \frac{\sigma_0}{\sigma(1+j\omega\tau)} \quad (2)$$

$$\sigma_0 = \frac{e^2 K_B T \tau}{\pi \hbar^2} \left[\frac{\mu_c}{K_B} + 2 \ln(1 + e^{-u_c/K_B T}) \right] \quad (3)$$

\hbar is reduced Planck's constant, K_B is Boltzmann's constant, T is the temperature, e is the electron charge, and μ_c is the chemical potential. $T=300K$ and $\tau = 0.1Ps$. Z_s is the surface impedance of the graphene, σ is the conductivity of the graphene.

B. Reconfigurable graphene antenna array

The radio technology of ultra-wideband (UWB) uses ultra-low transmitted energy for a high data rate over a large portion of the radio spectrum. The other definitions of UWB is when the antenna realizes bandwidth percentage greater than 25%. There are many wireless applications cover these spectrum as four/five generation of wireless communications. So, a reconfigurable operation is favored in these applications to cover and protect from channel fading and other losses.

Table 1: Dimensions of the 2×1 slot antenna array (all dimensions in mm)

L_{sub}	W_{sub}	100Ω	50Ω	W_f	L_g	W_{net}	R	W_{slot}
101	115	2	2.8	2.8	45	62	12.5	47
L_1	L_2	70Ω	Φ	W_s	W_1	W_2	L_{slot}	H
5	3	2.6	110°	9.5	5	3	51	0.8

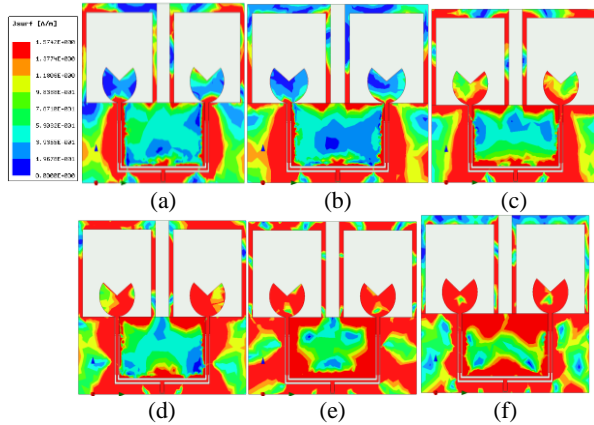


Fig. 4. (a)–(f) Surface current distribution for proposed 2×1 RSAA at 1.8, 2.1, 2.45, 3.5, 5.2 and 7 GHz, respectively.

Since UWB offers higher data rates with lesser multipath interference at lower power levels as compared to the narrow band communication systems as Shannon theorem [35]. So therefore the preferred band for implementation for many 4G and 5G wireless communication services. The operating band of the proposed antenna is extended by applying the DC voltage bias on the graphene layer as shown in Fig. 7.

IV. ANTENNA MEASUREMENT AND RESULTS

The proposed array is designed and all simulations are done by using finite element three dimensional

electromagnetic simulator, HFSS Ansys ver. 15 [29]. To verify the simulation results; the proposed antenna array element is fabricated and measured by using ZVA67 Rohde and Schwarz vector network analyzer from 10 MHz up to 67 GHz with different dc bias at 0 and 20 Volt as shown in Fig. 8 and by using bias Tee connector. Figure 9 and Fig. 10 present the comparison between simulated and measured reflection coefficient and voltage standing wave ratio (VSWR) variation versus frequency for the proposed RSAA at 0 and 20 Volt, respectively.

These figures indicate that good agreement is found between measured and simulated results. Figure 9 shows the performance at 0 Volt in which the $|S_{11}| < -10dB$ array impedance bandwidth extends from 1.7 to 2.5GHz, 3.3 to 3.8 GHz and 5 to 7 GHz. On the other hand, the impedance bandwidth extends from 1.5 GHz to 7 GHz with stop bands from 4 to 5 GHz at DC 20 Volt as shown in Fig. 10. These operating bands are suitable for RF energy harvesting at GPS, GSM, UMTS, Wi-Fi, LTE bands, and WMAX. The proposed array exhibits a nearly omnidirectional radiation pattern in the E and H-plane at 0 Volt graphene bias as indicated in Table 2. A comparison of the proposed 2×1 rectangular slot antenna array with other reported arrays is provided in Table 3.

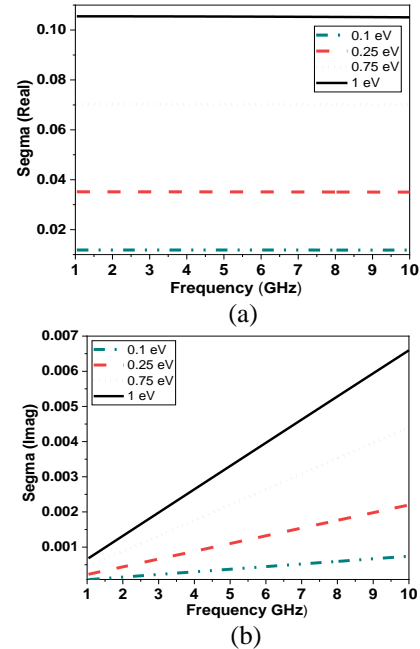


Fig. 5. The conductivity with frequency of the graphene at different bias voltage: (a) real and (b) imaginary part.

It can be deduced that the proposed array exhibits the ability to operate at most of 4G wireless communications and lower band of 5G frequency bands with increased gain and wider operating bandwidth by using single substrate. In addition to the simplicity of the array fabrication process.

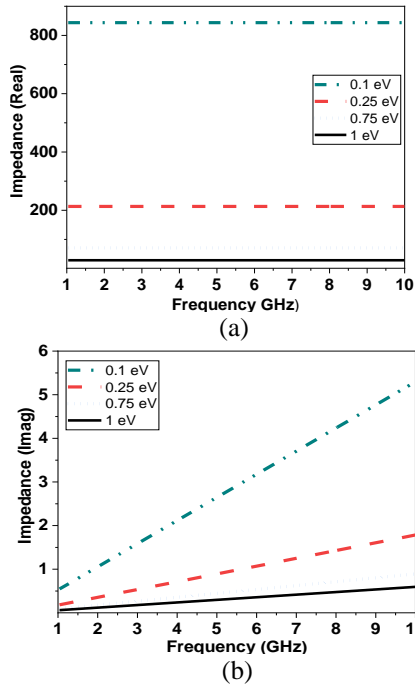


Fig. 6. The impedance with frequency of the graphene at different bias voltage: (a) real and (b) imaginary part.

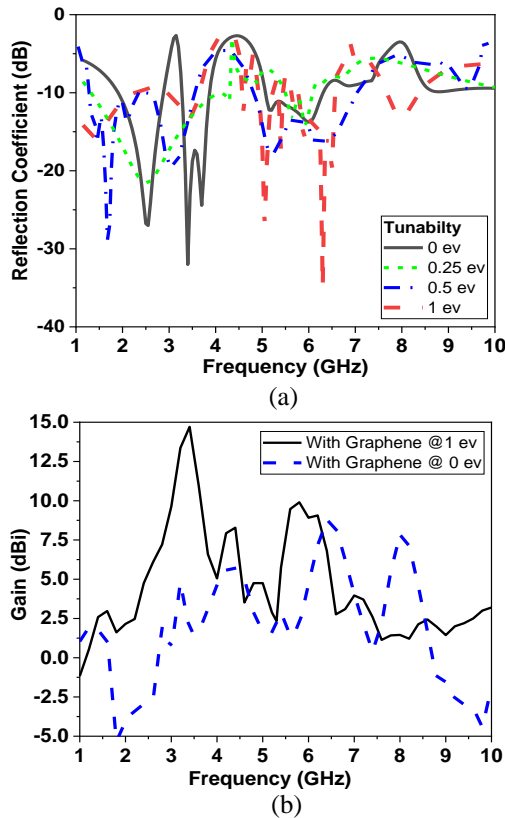


Fig. 7. Design procedures of the proposed array antenna with different graphene DC bias: (a) $|S_{11}|$ and (b) gain.

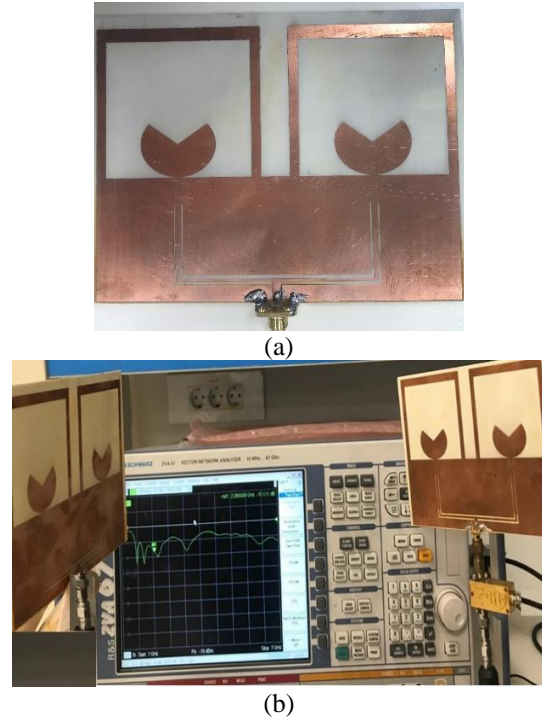


Fig. 8. Fabricated of RSAA: (a) photo of fabricated array and (b) setup measurement.

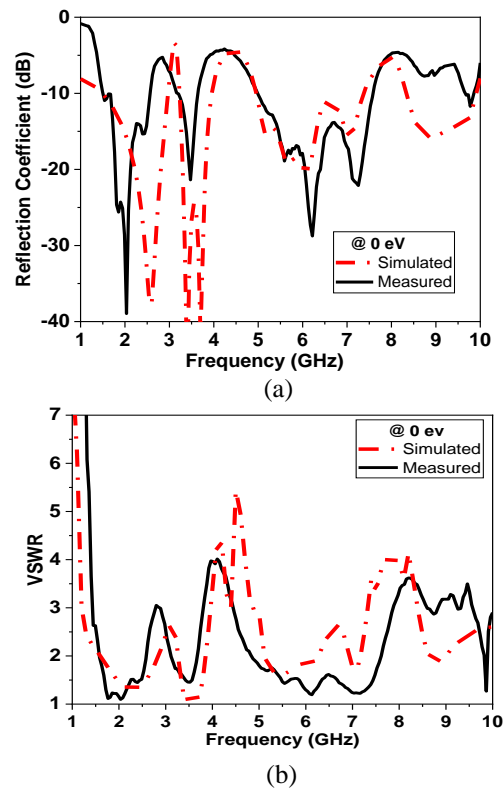


Fig. 9. The comparison between simulated and measured of RSAA at 0 Volt (a) $|S_{11}|$ and (b) VSWR.

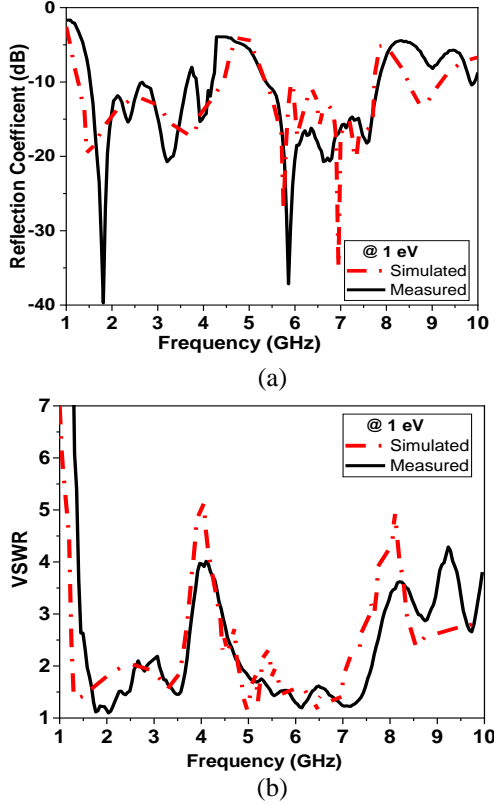
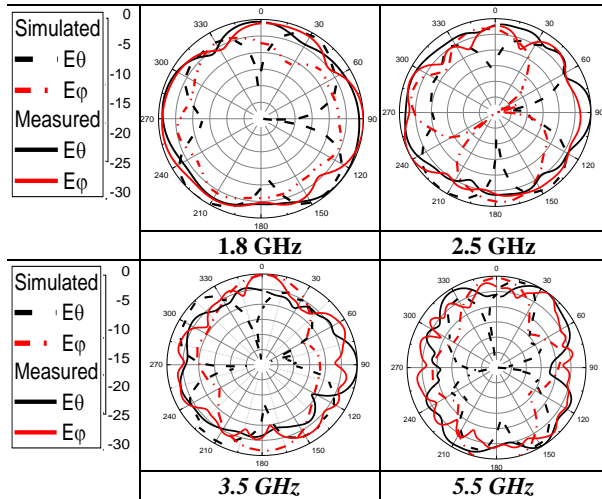


Fig. 10. The comparison between simulated and measured of RSAA at 20 Volt: (a) $|S_{11}|$ and (b) VSWR.

Table 2: Normalized simulated and measured radiation pattern E_θ and E_ϕ for the proposed 2×1 antenna array prototypes



V. RSAA APPLICATIONS

A. Group delay

Group delay is the serious parameter of design

UWB antenna for wireless communications since it could control the distortion of the transmitted pulses. The definition of the group delay is as the derivative with respect to frequency of the phase coupling between two identical UWB antennas $|S_{21}|$ [34-38]:

$$\tau = -\frac{\Delta\phi}{\Delta\omega} = -\frac{1}{360^\circ} \frac{d\phi(f)}{df} \tag{4}$$

The group delay should be close to a constant within the operation bands for perfect pulse transmission to obtain the phase linearity of the transmitted signals in the far field. The two antennas were aligned, and placed face to face orientation with separation distance greater than far field of the lowering operation bands as shown in Fig. 11 (a). The comparison results of $|S_{21}|$ for both measured and simulated HFSS results are shown in Fig. 11. Figure 11 (b) shows that the proposed antenna has perfect performance in this aspect and the group delay over the operating UWB band is less than 1 ns and the group delay and the magnitude transfer function are constant across the whole band except in the notched bands from 4 to 5 GHz. Thus, the proposed array is quite suitable for UWB wireless applications.

B. Object detection

By using face-to-face orientation as shown in Fig. 12 (a) and placement of objects with the same size and different materials as perfect conductor, polyethylene, and water in the far-field region, the magnitude and the convolution angle of the transmission coefficient $|S_{21}|$ between both rectangular slot antenna arrays are changed and they are plotted in Fig. 12 (b) and 12 (c). It is illustrated that the maximum transmission is achieved when the perfect conductor is placed. However, it gives a less commutative angle. On the other side the water produces highest transmission at 4.5 GHz and less transmission at frequency start from 6.5 GHz with largest commutative angle. Figure 13 shows the measured transmission coefficient magnitude and phase with three different objectives (perfect conductor, polyethylene and water) and compared with free space result.

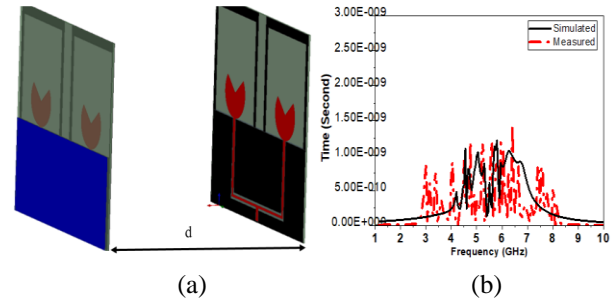


Fig. 11. Comparison between measured and simulated group delay of proposed 2×1 array antenna.

Table 3: Comparison with other reported 2×1 SR antenna arrays

Ref. Parameters	[36]	[37]	[38]	[39]	This Work
Bandwidth (GHz)	2—3.2	5.75—6.15	2.35—2.45	2.38—2.41	1.5—4 and 5—7
Array gain (dBi)	6.113 @ 2.65 GHz	10.77 @ 5.8 GHz	9.24 @ 2.4 GHz	9.22 @ 2.4 GHz	15 @ 3.5 GHz
Group delay	NM	NM	NM	NM	Less than 1 ns
No. of substrates	One	Two	One	One	One
Fabrication complexity	Simple	Complex	Simple	Simple	Simple
Feeding network	CPW	Microstrip	Microstrip	Microstrip	CPW
Tunability	Yes	No	No	No	Yes
Tuning mechanism	Graphene sheet	No	No	No	Graphene sheet layer
Object detection capability	No	No	No	No	Yes
Circuit size (mm ³)	101.88×77.64×0.813	130×80×1.53	180×140×1.6	110.5×83×1.56	115×101×0.8
Circuit size (λ_0) ³	0.9×0.68×0.007	2.51×1.54×0.03	1.44×1.12×0.013	0.88×0.66×0.0125	0.7×0.8×0.0064

NM: Not mention in the reference paper.

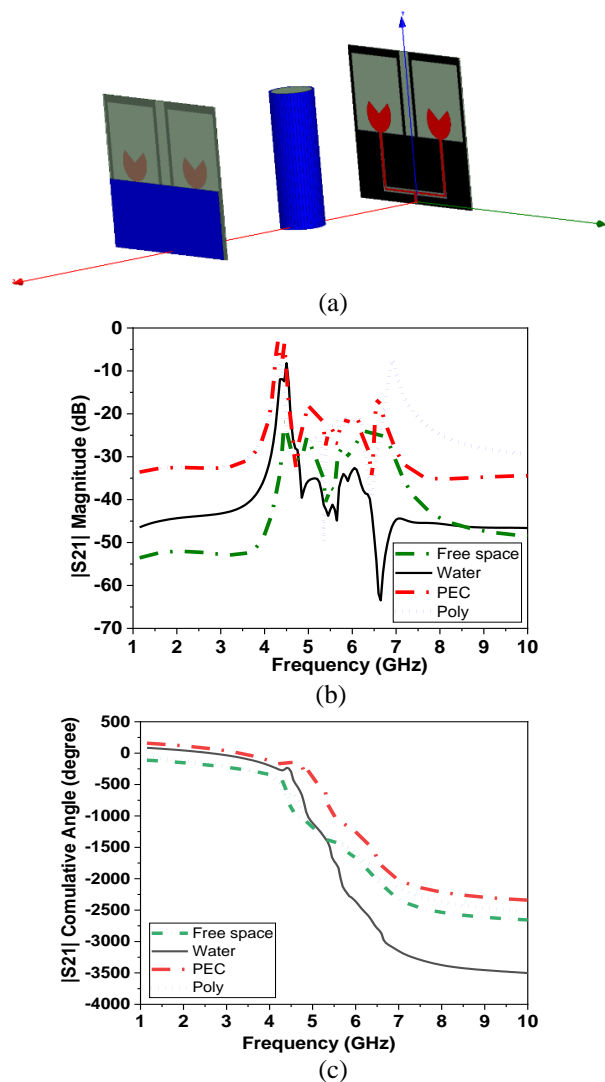


Fig. 12. (a) Simulated proposed array antenna detection system, (b) the $|S_{21}|$ transmission coefficient parameter magnitude, and (c) Phase commutative angle.

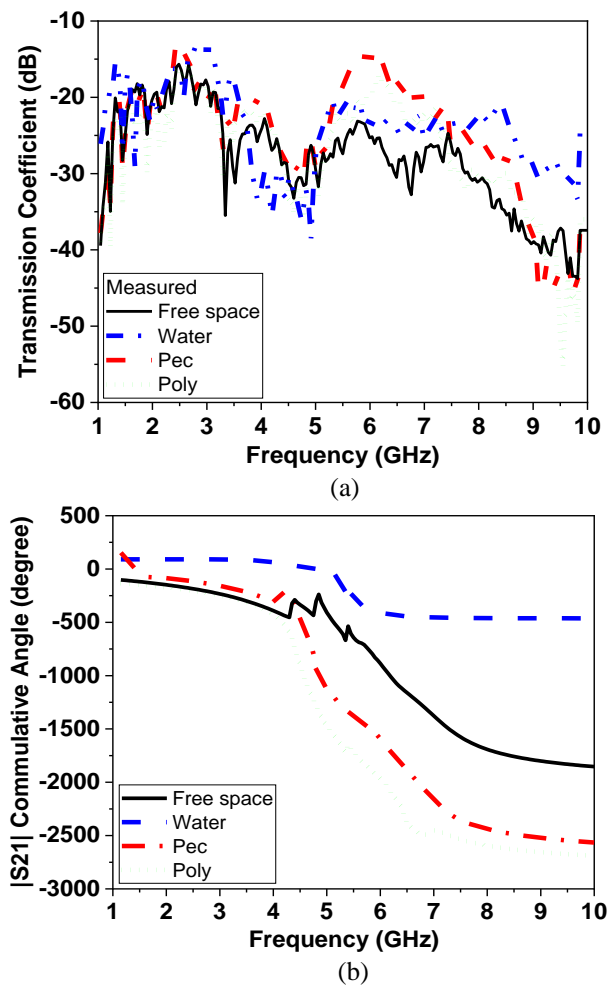


Fig. 13. Measured proposed array: (a) transmission coefficient magnitude, and (b) phase commutative angle.

VI. CONCLUSION

A CPW rectangular slot 2×1 antenna array is presented in this paper with a frequency range extending

from 1.7 to 2.5 GHz, 3.3 to 3.5 GHz, and from 5.5 to 5.8 GHz with an average gain of about 7.5 dBi over the operating bands. Graphene sheet layer was added on the other substrate side under the 2×1 rectangular slot array feeding network to realize reconfigurable frequency operation by changing the DC bias of the graphene layer. The lower band of 5G and other wireless communication bands. The operating frequency range extends from 1.5 to 3.5 GHz at the 4G bands and from 5 to 7 GHz at the lower band of 5G. The proposed antenna array acquires Omni-directional radiation pattern and improved gain values of 15 dBi by applying a 20 V bias voltage on the graphene layer. Experimental results have shown a range of reconfigurable and good agreement with the simulated results. The group delay of the proposed array is also studied with calculated values less than 1ns over the operating band. Moreover, the proposed array could be used to detect objects and to differentiate between different materials.

REFERENCES

- [1] M. Nejatijahromi, M. Rahman, and M. Naghshvarianjahromi, "Continuously tunable WiMAX band-notched UWB antenna with fixed WLAN notched band," *Progress Electromagnet. Res. Lett.*, vol. 75, pp. 97-103, 2018.
- [2] T. Li, H. Zhai, X. Wang, L. Li, and C. Liang, "Frequency reconfigurable bow-tie antenna for bluetooth, WiMAX, WLAN applications," *IEEE Antennas Wirel. Propag. Lett.*, vol. 14, pp. 171-4, 2015.
- [3] B. Zhang, K. Song, B. Xu, Z. Luo, and B. Hu, "Compact reconfigurable bandpass filter with wide frequency tuning range," *Electromagnetics*, vol. 39, no. 2, pp. 89-98, 2019.
- [4] A. A. Ibrahim, H. A. Mohamed, and W. A. E. Ali, "Tunable dual/triple band-pass filter based on stub-loaded resonators for wireless applications," *J. Instrum.*, vol. 12, no. 4, p. 04003, 2017.
- [5] A. Boutejdar, A. A. Ibrahim, and W. A. E. Ali, "Design of compact size and tunable band pass filter for WLAN applications," *Electron. Lett.*, vol. 52, no. 24, pp. 1996-7, 2016.
- [6] M. Peter and D. DiFilippo, "Multifunction RF systems for naval platforms," *Sensors*, vol. 18, 2018.
- [7] X. Huang, T. Leng, J. C. Chen, K. H. Chang, and Z. Hu, "Shielding effectiveness of screen printed graphene laminate at C band," *EuCAP'2016*, Davos, Switzerland, 2016.
- [8] H. A. Atallah, A. B. Abdel-Rahman, K. Yoshitomi and R. K. Pokharel, "Design of miniaturized reconfigurable slot antenna using varactor diodes for cognitive radio systems," in *Proceedings of the Fourth International Japan-Egypt Conference on Electronics, Communications and Computers (JEC-ECC)*, Cairo, pp. 63-66, 2016.
- [9] Y. Abdulraheem, G. Oguntala, A. Abdullah, H. Mohammed, R. Ali, R. Abd-Alhameed, and J. Noras, "Design of frequency reconfigurable multiband compact antenna using two PIN diodes for WLAN/WiMAX applications," *IET Microwaves, Antennas & Propagation*, vol. 11, no. 8, pp. 1098-1105, 2017.
- [10] V. Kumar, D. R. Jahagirdar, A. Basu, and S. K. Koul, "Intra-band frequency reconfigurable antenna using RF MEMS technology," in *Proceedings of the IEEE MTTT International Microwave and RF Conference*, New Delhi, pp. 1-4, 2013.
- [11] J. M. Floc'h and I. Ben Trad, "Printed planar double inverted-F antenna with large frequency reconfigurability range," in *Proceedings of the European Radar Conference (EURAD)*, Nuremberg, pp. 441-444, 2017.
- [12] X. I. Yang, J. C. Lin, G. Chen, and F. L. Kong, "Frequency reconfigurable antenna for wireless communications using GaAs FET switch," *IEEE Antennas and Wireless Propagation Letters*, vol. 14, pp. 807-810, 2015.
- [13] T. Leng, X. Huang, K. Chang, J. Chen, M. A. Abdalla, and Z. Hu, "Graphene nanoflakes printed flexible meanderedline dipole antenna on paper substrate for low-cost RFID and sensing applications," *IEEE Antennas Wireless Propag. Lett.*, vol. 15, pp. 1565-8, 2016.
- [14] X. Huang, Z. Hu, and P. Liu, "Graphene based tunable fractal Hilbert curve array broadband radar absorbing screen for radar cross section reduction," *AIP. Adv.*, vol. 4, no. 11, p. 117103, 2014.
- [15] G. W. Hanson, "Dyadic Green's functions for an anisotropic, non-local model of biased graphene," *IEEE Trans. Antennas Propag.*, vol. 56, no. 3, pp. 747-57, 2008.
- [16] D. Elsheakh "Reconfigurable frequency and steerable beam of monopole antenna based on graphene pads," *International Journal of RF and Microwave Computer-Aided Engineering*, vol. 30, Feb. 2020.
- [17] J. Jin, Z. Cheng, J. Chen, T. Zhou, C. Wu, and C. Xu, "Reconfigurable terahertz Vivaldi antenna based on a hybrid graphene-metal structure," *International Journal of RF and Microwave Computer-Aided Engineering*, vol. 30, Dec. 2020.
- [18] S. K. Yadav, A. Kaur, and R. Khanna, "An ultra-wideband "OM" shaped DRA with a defected ground structure and dual polarization properties for 4G/5G wireless communications," *International Journal of RF and Microwave Computer-Aided Engineering*, vol. 30, 2020.
- [19] J. Zhang, Z. Liu, W. Lu, H. Chen, B. Wu, and Q. Liu, "A low profile tunable microwave absorber based on graphene sandwich structure and high impedance surface," vol. 30, 2020.

- [20] X. Zhou, J. Le Kernec, and D. Gray, "Vivaldi antenna for railway cutting monitoring," *2016 CIE International Conference on Radar (RADAR)*, Guangzhou, pp. 1-5, 2016.
- [21] G. W. Hanson, "Dyadic Green's functions for an anisotropic, non-local model of biased graphene," *IEEE Trans. on Antennas Propag.*, vol. 56, no. 3, pp. 747-757, 2008.
- [22] D. Elsheakh, and E. Abdallah, "Ultra-wide-bandwidth (UWB) microstrip monopole antenna using split ring resonator (SRR) structure," *International Journal of Microwave and Wireless Technologies*, vol. 10, no. 1, pp. 123-132.
- [23] A. A. A. Aziz, M. A. Abdalla, and A. A. Ibrahim, "Enhanced gain tunable two elements antenna array based on graphene," *2018 IEEE International Symposium on Antennas and Propagation & USNC/URSI National Radio Science Meeting*, Boston, MA, pp. 471-472, 2018.
- [24] E. S. Angelopoulos, A. Z. Anastopoulos, D. I. Kaklamani, A. A. Alexandridis, F. Lazarakis, and K. Dangakis, "Circular and elliptical CPW-fed slot and Microstrip-Fed antennas for ultrawideband applications," in *IEEE Antennas and Wireless Propagation Letters*, vol. 5, pp. 294-297, 2006.
- [25] Q. Ayn, P. A. Nageswar Rao, and P. Mallikarjuna Rao, "Design and analysis of high gain 2x1, 4x1, 8x1 and 8x8 circular patch antenna arrays for 2.4 GHz applications," *International Journal of Innovative Research in Science, Engineering and Technology*, vol. 6, no. 8, Aug. 2017.
- [26] M. Niamien, S. Collardey, A. Sharaiha, and K. Mahdjoubi, "An electrically small frequency reconfigurable antenna for DVB-H," *IEEE Int. Workshop Antenna Technol.*, p. 245248, 2012.
- [27] S. Wu, D. Zha, Y. He, L. Miao, and J. Jiang, "Design of a tunable absorber based on graphene in the THz range," *2019 IEEE International Conference on Computational Electromagnetics (ICCEM)*, Shanghai, China, pp. 1-3, 2019.
- [28] C. Fan, B. Wu, Y. Hu, Y. Zhao, and T. Su, "Millimeter-wave pattern reconfigurable Vivaldi antenna using tunable resistor based on graphene," in *IEEE Transactions on Antennas and Propagation*, vol. 68, no. 6, pp. 4939-4943, June 2020.
- [29] www.ansys.com
- [30] A. Q. Zhang, Z. G. Liu, L. Wei-Bing, and H. Chen, "Graphene-based dynamically tunable attenuator on a coplanar waveguide or a slotline," *IEEE Trans. Microw. Theory Techn.*, vol. 67, no. 1, pp. 70-77, Jan. 2019.
- [31] A. K. Geim and K. S. Novoselov, "The rise of graphene," *Nat. Mater.*, vol. 6, pp. 183-91, 2007.
- [32] L. H. Jui, L. Yinying, D. Huilian, S. Poman, and B. Jens, "Time-domain modelling of group-delay and amplitude characteristics in ultra-wideband printed-circuit antennas," 10.1007/978-3-540-68768-9_19, 2008.
- [33] D. Zhao, C. Yang, M. Zhu, and Z. Chen, "Design of WLAN/LTE/UWB antenna with improved pattern uniformity using ground-cooperative radiating structure," in *IEEE Transactions on Antennas and Propagation*, vol. 64, no. 1, pp. 271-276, Jan. 2016.
- [34] J. Wu, Z. Zhao, Z. Nie, and Q. Liu, "A printed UWB Vivaldi antenna using stepped connection structure between slot line and tapered patches," in *IEEE Antennas and Wireless Propagation Letters*, vol. 13, pp. 698-701, 2014.
- [35] <https://www.sciencedirect.com/topics/computer-science/shannon-sampling-theorem>
- [36] A. A. A. Aziz, M. A. Abdalla, and A. A. Ibrahim, "Enhanced gain tunable two elements antenna array based on graphene," *2018 IEEE International Symposium on Antennas and Propagation & USNC/URSI National Radio Science Meeting*, Boston, MA, USA, pp. 471-472, 2018.
- [37] N. Husna, M. A. Jamlos, W. A. Mustafa, and S. Z. S. Idrus, "High gain of 2x1 simulated circularly polarized rectangular microstrip patch array antenna," *International Conference on Technology, Engineering and Sciences (ICTES)*, pp. 1-6, 2020.
- [38] A. B. Obot, G. A. Igwe, and K. M. Udofia, "Design and simulation of rectangular microstrip antenna arrays for improved gain performance," *International Journal of Networks and Communications*, vol. 9, no. 2, pp. 73-81, 2019.
- [39] A. El Alami, Y. Ghzaoui, S. Das, S. D. Bennani, and M. El Ghzaoui, "Design and simulation of RFID array antenna 2x1 for detection system of objects or living things in motion," *International Workshop on Microwave Engineering, Communications Systems and Technologies (MECST)*, Leuven, Belgium, pp. 1010-1015, 2019.